EXPERIMENTAL INVESTIGATIONS ON HEAT TRANSFER TO CO₂ FLOWING UPWARD IN A NARROW ANNULUS AT SUPERCRITICAL PRESSURES

HWAN YEOL KIM*, HYUNGRAE KIM, DEOG JI KANG, JIN HO SONG and YOON YEONG BAE
Korea Atomic Energy Research Institute
105 Duckjin-Dong, Yuseong-Gu, Daejeon 305-353, Korea
*Corresponding author. E-mail : hykim1@kaeri.re.kr

Heat transfer experiments in an annulus passage were performed using SPHINX (*S*upercritical *P*ressure *H*eat Transfer *I*nvestigation for *NeX*t Generation), which was constructed at KAERI (Korea Atomic Energy Research Institute), to investigate the heat transfer behaviors of supercritical CO₂. CO₂ was selected as the working fluid to utilize its low critical pressure and temperature when compared with water. The mass flux was in the range of 400 to 1200 kg/m² s and the heat flux was chosen at rates up to 150 kW/m². The selected pressures were 7.75 and 8.12 MPa. At lower mass fluxes, heat transfer deterioration occurs if the heat flux increases beyond a certain value. Comparison with the tube test results showed that the degree of heat transfer deterioration in the heat flux was smaller than that in the tube. In addition, the Nusselt number correlation for a normal heat transfer mode is presented.

1. INTRODUCTION

The SCWR (SuperCritical Water-cooled Reactor) is a Generation IV reactor selected by the GIF (Generation IV International Forum) for development since it has a higher thermal efficiency than the existing nuclear power plants and has an enhanced economical potential. The SCWR is considered to be a feasible concept for an innovative nuclear power plant if the existing technologies developed for the supercritical pressure fossil plants, BWRs, and PWRs are used together with additional researches in several areas such as materials, water chemistry, and safety. Among the various research areas, heat transfer experiments under supercritical conditions are required for proper prediction of the thermal hydraulic phenomena in the reactor core.

The thermal-hydraulic characteristics of a supercritical pressure fluid are different from those of a subcritical pressure fluid, since the physical properties of a supercritical fluid change drastically near a pseudo-critical temperature [1]. Due to this variation, heat transfer efficiency also changes considerably depending on flow conditions. Thus, a SCWR design requires a reliable database of thermal-hydraulic characteristics of supercritical water flows in the proposed geometries and operation conditions.

A heat transfer test facility, SPHINX (*S*upercritical Pressure *H*eat Transfer *I*nvestigation for *NeX*t Generation), was constructed at KAERI (*K*orea *A*tomic *E*nergy *R*esearch *I*nstitute) to investigate the thermal-hydraulic behaviors of supercritical CO₂ at several test sections with different geometries. The loop uses CO₂ as a surrogate fluid for water since the critical pressure (7.38 MPa) and temperature (31.05 °C) of CO₂ are much lower than those of water (22.12 MPa and 374.14 °C), and these two fluids show similar physical property characteristics near the pseudo-critical temperature [1].

Heat transfer experiments were performed using SPHINX to investigate the characteristics of a heat transfer in supercritical CO₂, which was flowing upward through a narrow annulus passage at supercritical pressures. In the test section, an unheated outer housing tube with an inside diameter of 10.0 mm surrounded a heated inner rod with an outside diameter of 8.0 mm. The heated length of the test section was 1800 mm. The supercritical pressure CO₂ passed through a narrow gap of 1.0 mm. Twelve thermocouples were installed on the surface of the heated inner rod. The mass flux and heat flux changed at a given system pressure. The experimental results were analyzed and compared with the results from previous research performed in a tube with an inside diameter of 4.4 mm [2,3].

2. EXPERIMENTAL APPARATUS AND METHOD

2.1 Description of SPHINX

Figure 1 shows a schematic diagram of SPHINX, which is designed to accommodate various geometries for test sections, such as a single tube, a single rod, and a rod bundle, using supercritical CO_2. The design pressure of the main loop is 12.0 MPa. The supercritical CO_2 remains in a liquid-like state from the outlet of the cooler to the inlet of the test section. The liquid-like supercritical CO_2 becomes a gas-like supercritical CO_2 as it flows through the heated test section. Thereafter, the supercritical CO_2 remains in a gas-like state up to the inlet of the cooler.

Two units of CO_2 circulation pumps were installed. The lower capacity unit was for the single tube and single rod tests, and the higher capacity unit was for the rod bundle tests. A gear-type circulation pump was used to minimize the flow fluctuations. An accumulator filled with gaseous nitrogen was installed downstream of the pumps to control the main loop pressure and to absorb the pressure fluctuations. An electric pre-heater was provided to control the fluid temperature at the inlet of the test section, and an AC power supply was provided to control the heat flux at the test section. The mass flow rate was regulated by adjusting the bypass valve and/or the speed of the pumps. A compact spiral-type cooler was provided to cool the supercritical CO_2. In addition, an auxiliary chiller system was also installed to feed chilled coolant into the cooler. A pressure relieving device (PSV) was used to prevent over-pressurization of the main loop. An air-driven boosting compressor was used for the initial charge of CO_2 from the CO_2 tank into the main loop. A Corioli-type

flow meter, manually operated bypass and isolation valves, venting valves, pressure transmitters, and K-type thermocouples were installed in the main loop. The main loop was insulated to minimize heat loss to the environment. The inside diameter of the main loop pipe was approximately 20 mm. The accuracy and range of the instruments in the main loop are shown in Table 1.

2.2 Test Section

Figure 2 shows a sketch of the annulus passage test section which was internally heated by the heater rod. In the test section, an unheated outer housing tube with an inside diameter of 10.0 mm surrounded the heated inner rod with an outside diameter of 8.0 mm. The heated length of the test section was 1800 mm. The inner rod with an Inconel 600 sheath was heated by passing an alternating current through the internal heater element and held coaxially with the outer tube by cell stops placed axially at 200 mm intervals. Twelve thermocouples were installed on the surface of the heater rod to measure

Table 1. Accuracy and Range of Measuring Instruments

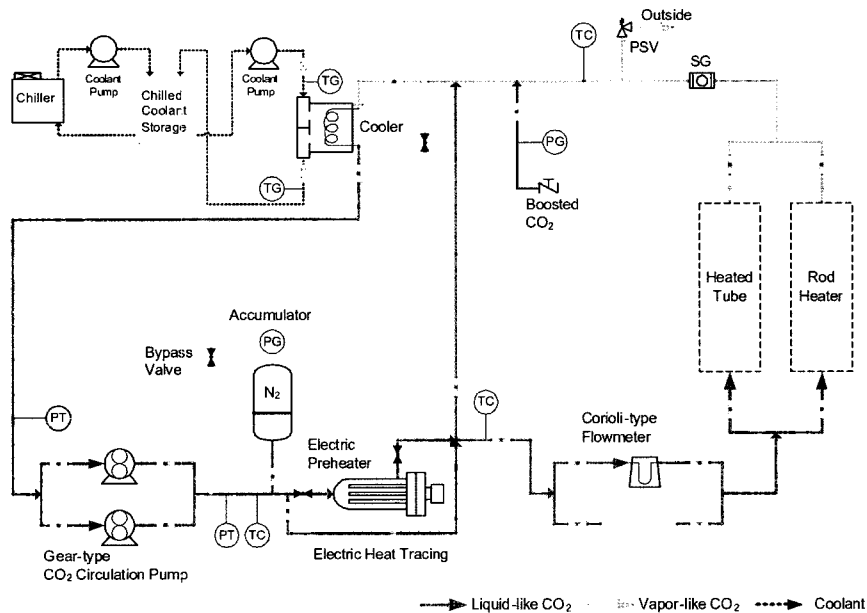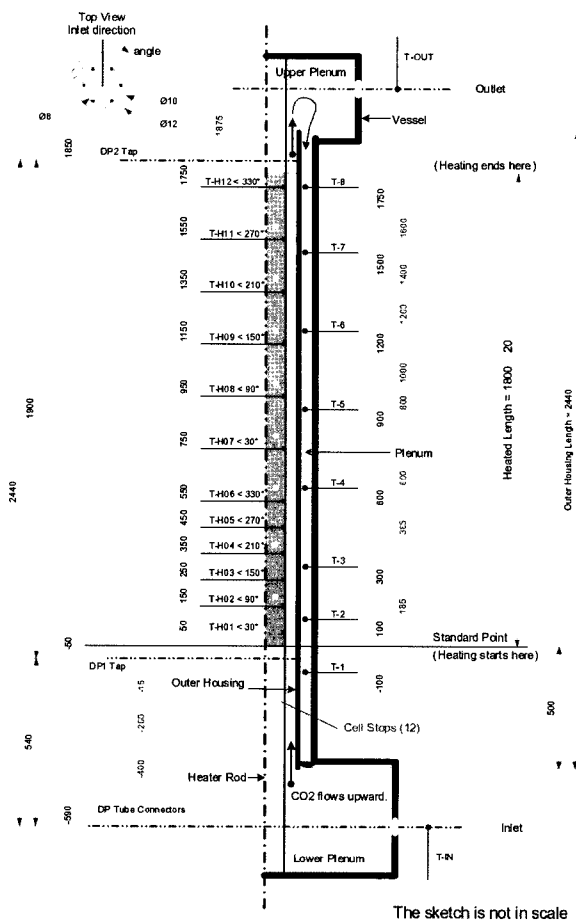| Measuring instrument	Accuracy	Range
K-type thermocouple	±0.75 % of span or ± 2.2 °C	0 ~ 1260 °C
Pressure transmitter	±0.25 % of span	0 ~ 16 MPa
Mass flow meter	± 0.15 %	0 ~ 680 kg/hr

Fig. 1. Schematic Diagram of SPHINX

Fig. 2. Sketch of the Annular Test Section

of the fluid and the imposed heat flux. The heat transfer coefficient, h, was calculated from the measured surface temperature of the heater rod, the given heat flux, and the estimated bulk fluid temperature as follows.

$$h = \frac{q''}{\left(T_w - T_b\right)} \tag{1}$$

The control parameters in the experiments were the inlet pressure, inlet fluid temperature, wall heat flux, and mass flux. The wall heat flux and mass flux were manipulated by changing the AC power supplied to the test section and the mass flow rate through the test sections. The inlet pressure was measured at the pressure tap for the annulus.

The equivalent thermal diameter of the annulus passage, which was calculated based on the heated perimeter, was 4.5 mm, which is nearly the same as the inside diameter of the tube (i.e. 4.4 mm) used in the previous tests.

2.3 Test Conditions

The loop was designed to perform various experiments including the test matrix where the inlet Re number of the test section was 50,000, which was the design value at the core inlet of the SCWR proposed in Tokyo University [2]. The experiment was performed by varying the mass flux, heat flux, inlet pressure, and inlet temperature. The mass flux was selected to include the Re number of 50,000 at the inlet of the test section. The heat flux was selected so that the test data in the pseudo-critical conditions could be measured to investigate the heat transfer deteriorations. The ranges of the controlled parameters were 400 to 1200 kg/m² s for the mass flux, up to 150 kW/m² for the heat flux, 7.75 and 8.12 MPa for the inlet pressure, and 0 ~ 37 °C for the inlet temperature. Table 2 summarizes the test conditions.

surface temperatures of up to 650 °C. The accuracy of the thermocouple was ±0.4% of the measured temperature. The first and last thermocouples were installed 50 mm from the lower and upper ends of the heater rod to avoid interference from the unheated sections of the heater rod. Six thermocouples in the lower part of the heater rod were equally spaced 100 mm apart and each thermocouple was circumferentially separated by 60°. The other six thermocouples in the upper section of the heater rod were equally spaced 200 mm apart and each thermocouple was also circumferentially separated by 60°. The thermocouple diameter was 0.5 mm. The thermocouples were installed on the surface of the heater rod where small grooves were carved. Since the sizes of the thermocouples and grooves were small, it is believed that the installed thermocouples do not have an impact on the flow and temperature fields.

The test section was insulated to minimize heat loss to the environment. The test section maintained a constant wall heat flux along its heated length. The bulk fluid temperature in the passage was estimated from a heat balancing formula using the measured inlet temperature

Table 2. Test Conditions

Parameter	Unit	Value
Inlet pressure	MPa	7.75, 8.12 (1.05, 1.1P$_{crit}$ respectively)*
Inlet temperature	°C	0 ~ 37
Mass flux	kg/m² s	400 ~ 1200
Heat flux	kW/m²	Up to 150

3. RESULTS AND DISCUSSION

3.1 Wall Temperature and Heat Transfer Coefficient

Figures 3 and 4 show the measured wall temperatures and the heat transfer coefficients versus the bulk fluid

enthalpy at inlet pressures of 7.75 MPa and 8.12 MPa, respectively. The tests were performed with various mass fluxes and heat fluxes.

At the given mass flux and heat flux, several tests were conducted with varying inlet temperatures. Thus, there may be some overlap in the heat transfer coefficient and
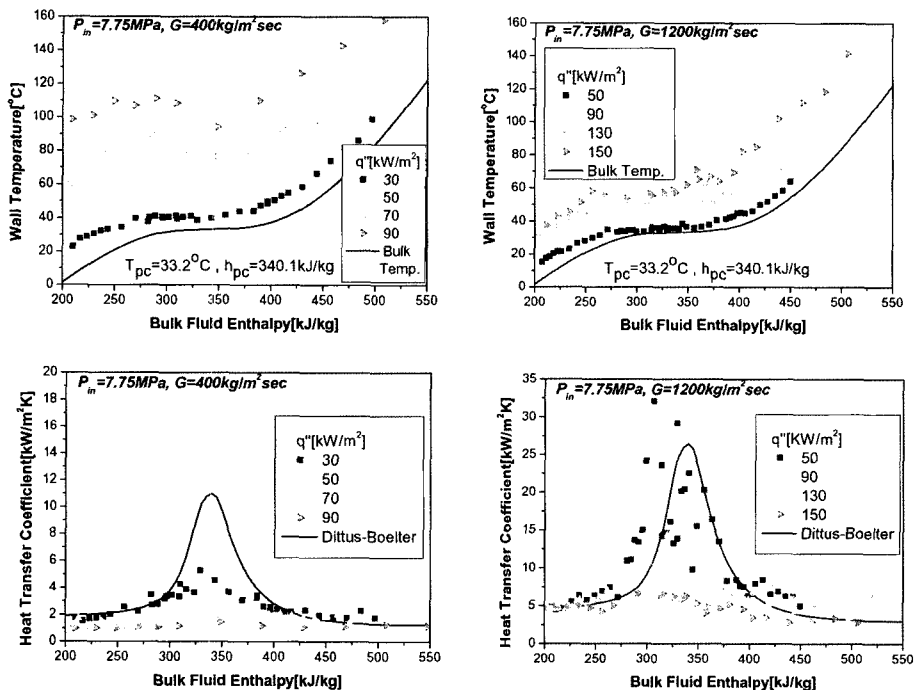

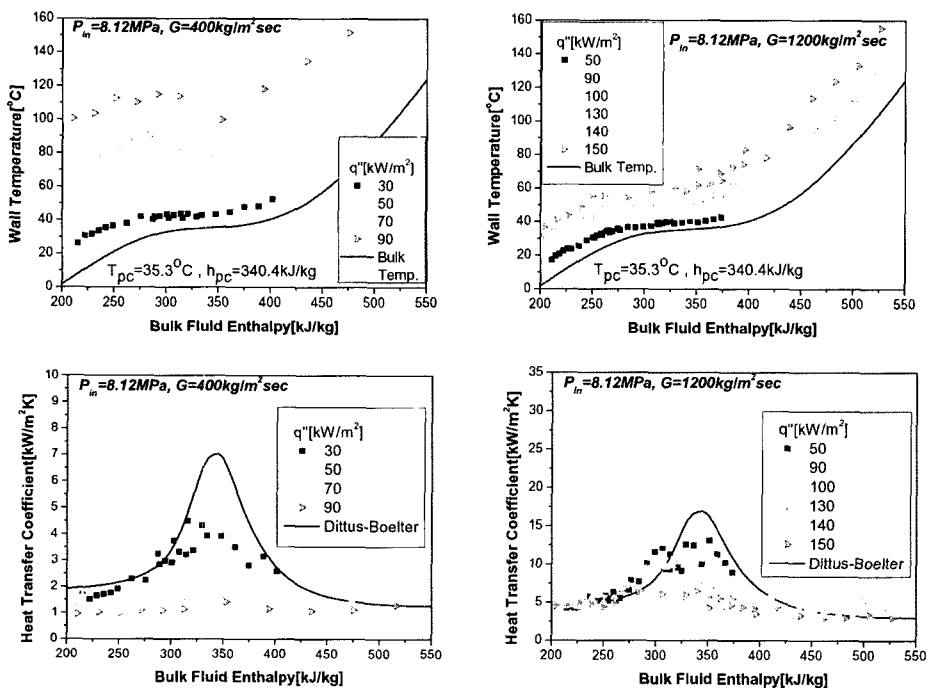Fig. 3. Heat Transfer Coefficient and Wall Temperature at an Inlet Pressure of 7.75 MPa

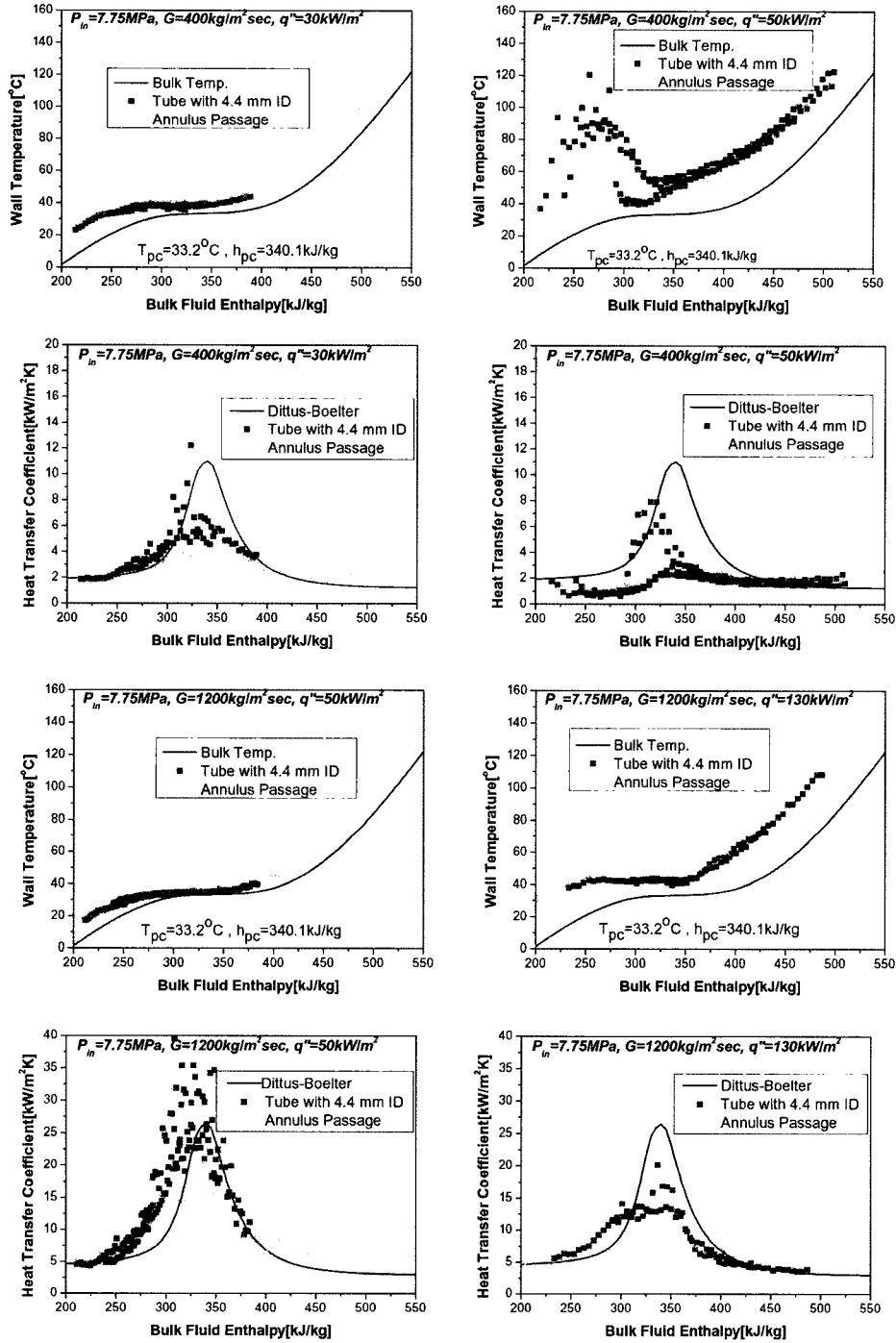Fig. 4. Heat Transfer Coefficient and Wall Temperature at an Inlet Pressure of 8.12 MPa

Fig. 5. Comparison with Tube Test at an Inlet Pressure of 7.75 MPa

wall temperature at the same mass flux and heat flux. The solid black line is the heat transfer coefficient calculated from the following Dittus-Boelter correlation [4]:

$$Nu_b = \frac{hD}{k_b} = 0.023 Re_b^{0.8} Pr_b^{0.4} . \qquad (2)$$

At the same mass flux, the wall temperature increased as the heat flux increased. This resulted in a decrease in the heat transfer coefficient. At a lower mass flux (G = 400 kg/m² s), heat transfer deterioration occurred if the heat flux increased (i.e. q" ≥ 50 kW/m²). At a higher mass flux (G = 1200 kg/m² s), a slight heat transfer deterioration occurred at the highest heat flux (i.e. q" = 150 kW/m²). It

is noticeable that heat transfer deterioration occurred where the bulk fluid enthalpy was lower than the pseudo-critical enthalpy, and the maximum heat transfer coefficient occurred where the bulk fluid enthalpy was slightly lower than the pseudo-critical enthalpy. It was also observed that the heat transfer coefficient was scattered when the pressure was close to the critical pressure and/or the wall temperature was close to the fluid temperature. The temperature difference between the wall and the fluid was small when the mass flux was high at a low heat flux or the fluid condition was near a pseudo-critical temperature. It remains uncertain whether the scattering of the data is due to an uncertainty in the measurements of the wall temperature and the inlet fluid temperature or an unidentified flow instability near the critical pressure.

It is interesting to note that the heat transfer coefficients were very close to the ones predicted using the Dittus-Boelter correlation in a region far from the pseudo-critical region. However, the prediction begins to deviate from the measured values as the fluid temperature approaches the pseudo-critical temperature.

3.2 Comparison with Tube Test Results

Heat transfer tests had been performed previously for a vertical single tube with an inside diameter of 4.4 mm, where the supercritical CO_2 flowed upward, for various mass and heat fluxes [2,3] The thermal equivalent diameter of the annulus passage, which was calculated based on the heated perimeter, is 4.5 mm and was almost identical to the inside diameter of the tube (i.e. 4.4 mm). Figures 5 and 6 show a comparison of the test results with the results from the previous tests performed in a tube with an inside diameter of 4.4 mm at inlet pressures of 7.75 MPa and 8.12 MPa, respectively. It was assumed that the heat transfer coefficient obtained from the Dittus -Boelter correlation was the same for the annulus passage and the tube. It is shown that heat transfer deterioration occurs when G = 400 kg/m^2 s and q" = 50 kW/m^2 for both the annulus passage and the tube. It was also observed that the degree of heat transfer deterioration for the annulus passage was smaller than that for the tube. In the deteriorated region, the heat transfer coefficient for the annulus passage was slightly higher than that for the tube. A similar trend was also observed in the tests performed with R22 as working fluid [5]. This suppression of heat transfer deterioration for the annulus passage may be caused by a different mechanism for heat transfer deterioration from that for the tube. The interaction of a wall frictional force and a buoyancy force affects the cross-sectional velocity profile and is considered to be a major factor for heat transfer deterioration. It seems that the smaller flow gap of the annulus passage, when compared with that of the tube, may produce an interaction between the wall frictional force and the buoyancy force, which is quite different from the tube. If this is true, it is recommended that a different equivalent diameter is used for a direct comparison of the

test results between the annulus passage and the tube. For a normal heat transfer, however, the heat transfer coefficient for the annulus passage is similar to that of the tube.

4. HEAT TRANSFER CORRELATION

The experimental data for G = 400 kg/m^2 s and 1200 kg/m^2 s were analyzed to obtain a Nusselt number correlation by considering not only a forced convection but also a mixed convection where the effect of buoyancy is incorporated as a function of the buoyancy parameters. The data in the range of the heat transfer deterioration mode (q" = 50, 70, and 90 kW/m^2 for G = 400 kg/m^2 s and q" = 150 kW/m^2 for G = 1200 kg/m^2 s) were excluded in the generation of the correlation because they resulted in many discrepancies between the measured and predicted data. The Nusselt number takes the forms as shown in Eqs. (3) - (6).

$$Nu_b = Nu_{var} \cdot f(B), \quad B = \frac{\overline{Gr}}{Re_b^{2.7} \overline{Pr}^{0.5}} \quad (3)$$

$$Nu_{var} = 0.0183 Re_b^{0.82} Pr_b^{0.5} \left(\frac{\rho_w}{\rho_b}\right)^{0.3} \left(\frac{\overline{c_p}}{c_{pb}}\right)^n \quad (4)$$

$$n = \begin{cases} 0.4 \ for \ \frac{T_b}{T_{pc}} < \frac{T_w}{T_{pc}} \leq 1 \ or \ 1.2 \leq \frac{T_b}{T_{pc}} < \frac{T_w}{T_{pc}} \\ 0.4 + 0.2\left(\frac{T_w}{T_{pc}} - 1\right) \ for \ \frac{T_b}{T_{pc}} \leq 1 < \frac{T_w}{T_{pc}} \\ 0.4 + 0.2\left(\frac{T_w}{T_{pc}} - 1\right)\left[1 - 5\left(\frac{T_b}{T_{pc}} - 1\right)\right] \ for \ 1 < \frac{T_b}{T_{pc}} < 1.2 \ and \ \frac{T_b}{T_{pc}} < \frac{T_w}{T_{pc}} \end{cases} \quad (5)$$

$$f(B) = \begin{cases} \left(0.8 + 6.0 \times 10^6 B\right)^{-0.8} \ for \ B \leq 7.0 \times 10^{-8} \\ 0.261 + 3.068 \times B^{0.1} \ for \ 7.0 \times 10^{-8} < B \leq 7.0 \times 10^{-7} \\ 1.47 - 6.7 \times 10^5 B \ for \ 7.0 \times 10^{-7} < B \leq 1.0 \times 10^{-6} \\ 0.8 \ for \ 1.0 \times 10^{-6} < B \leq 1.0 \times 10^{-5} \\ 0.1423 \times B^{-0.15} \ for \ 1.0 \times 10^{-5} < B \end{cases} \quad (6)$$

Figure 7 shows a comparison of the measured and predicted heat transfer coefficients based on Eqs. (3) – (6). Most of the data are within the error bound of +/- 30%.

5. CONCLUSIONS

Heat transfer experiments were performed to investigate the characteristics of a heat transfer to CO_2 which passed upward through a narrow annulus passage at supercritical
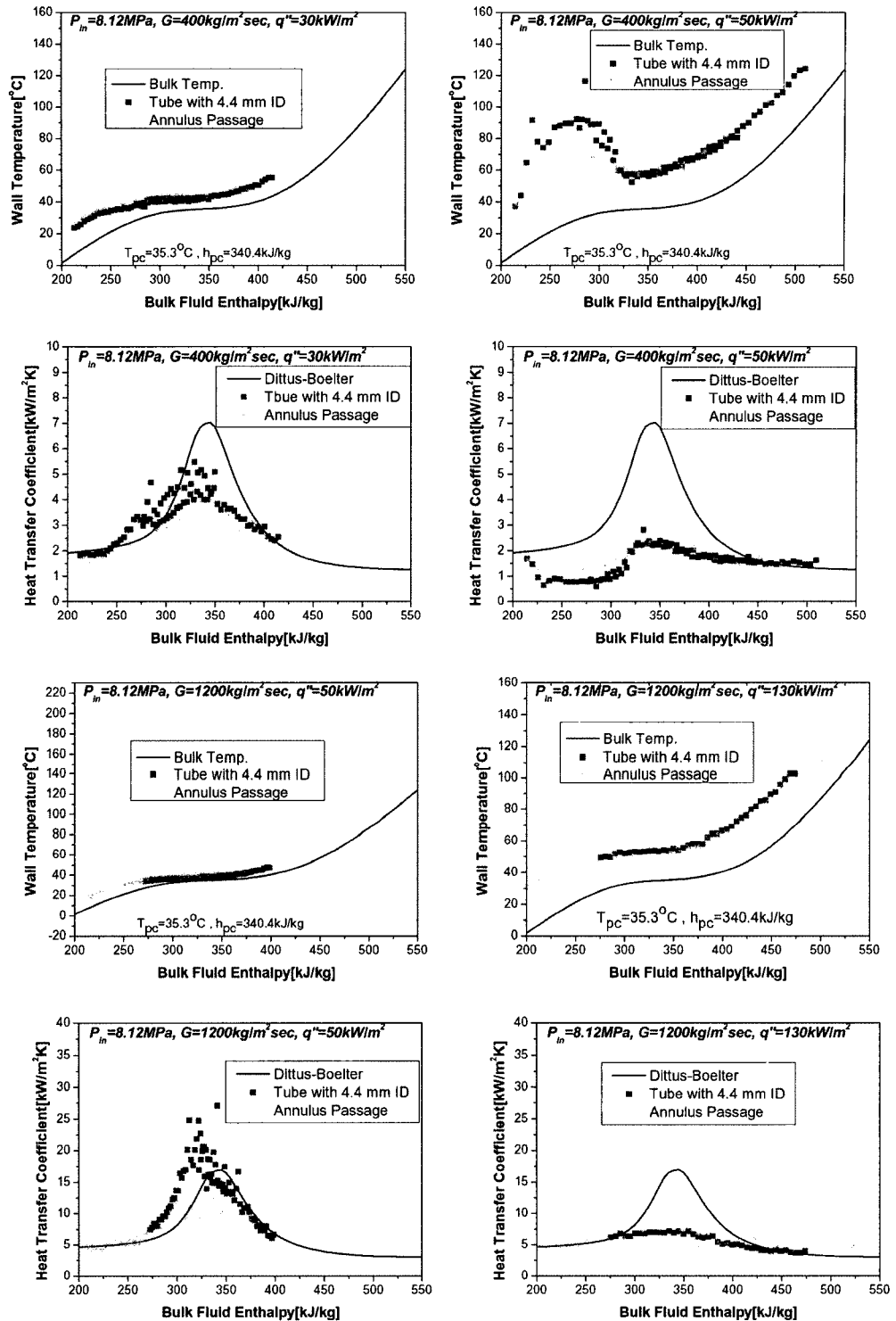
Fig. 6. Comparison with Tube Test at an Inlet Pressure of 8.12 MPa

pressures. The mass fluxes and heat fluxes changed at a given pressure. At the same mass flux, the heat transfer coefficient increased as the heat flux increased. At a lower mass flux ($G = 400$ kg/m^2 s), heat transfer deterioration occurred if the heat flux exceeded 50 kW/m^2. At a higher mass flux ($G = 1200$ kg/m^2 s), a
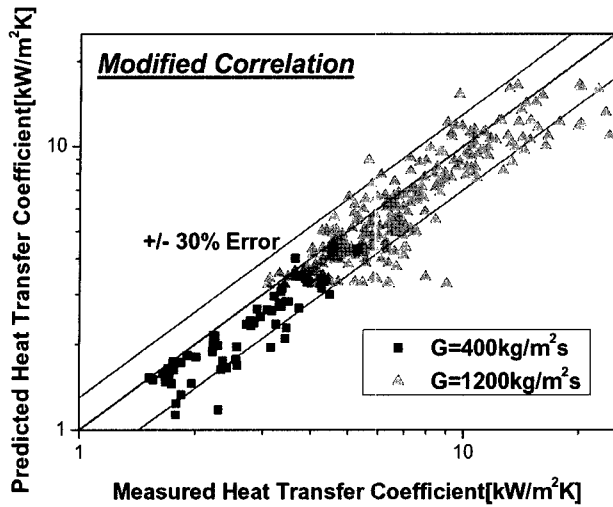
Fig. 7. Comparison of Measured and Predicted Heat Transfer Coefficients

slight heat transfer deterioration occurred at the highest heat flux (i.e. q" = 150 kW/m²). Comparison with the tube test results showed that a suppression of the heat transfer deterioration occurs, which may be caused by a smaller flow gap. For a normal heat transfer, however, the heat transfer coefficient is similar to that in a tube. The Nusselt number correlation is presented based on the data in the range of a normal heat transfer mode.

ACKNOWLEDGEMENTS

Nomenclature

c_p specific heat capacity [kJ/kg · K]
$\overline{C_p}$ averaged specific heat capacity, $(i_w\text{-}i_b)/(T_w\text{-}T_b)$
  [kJ/kg · K]
D hydraulic diameter [m]
h heat transfer coefficient [kW/m · K]
i specific enthalpy [kJ/kg]
k thermal conductivity [kW/m²K]
G mass flux [kg/m²s]
Gr Grashof number, $\rho_b(\rho_b\text{-}\rho_w)gD^3/\mu_b^2$
  Grashof number with rm, ρ_m, $\rho_b(\rho_b\text{-}\rho_m)gD^3/\mu_b^2$
Nu Nusselt number

Re Reynolds number
$\overline{Pr}$ Prandtl number
$\overline{Pr}$ Prandtl number with $\overline{c_p}$
P pressure [MPa]
$q"$ heat flux at the wall [kW/m²]
T temperature [K]

Greek Letters

μ dynamic viscosity [Pa · s]
ρ density [kg/m³]
ρ_m averaged density, $\dfrac{1}{T_w - T_b}\int_{T_b}^{T_w}\rho dT$ [kg/m³]

Subscripts

b property at bulk fluid temperature
cr critical point
pc property at pseudo-critical temperature
w property at wall temperature

REFERENCES

[1] H. Y. Kim et al., State of the Art on the Heat Transfer Experiments Under Supercritical Pressure Condition, KAERI/AR-681/2003 (2003).

[2] H. Y. Kim, H. Kim, J. H. Song, B. H. Cho, and Y. Y. Bae, "Heat Transfer Test in a Vertical Tube Using CO₂ at Supercritical Pressures," J. Nucl. Sci. Technol., Vol. 44, No. 3, 285-293 (2007).

[3] H. Kim, Y. Y. Bae, H. Y. Kim, J. H. Song, and B. H. Cho, "Experimental Investigation on the Heat Transfer Characteristics in a Vertical Upward Flow of Supercritical CO₂," Proc. ICAPP' 06, Paper 6123, Reno, NV USA, June 4-8, 372-381 (2006).

[4] F. P. Incropera, D. P. Dewitt, T. L. Bergman, and A. S. Lavine, Introduction to Heat Transfer, 5ᵗʰ ed., p. 484, John Wiley & Sons (2007).

[5] H. Mori, S. Yoshida, S. Morooka, and H. Komita, "Heat Transfer Study Under Supercritical Pressure Conditions for Single Rod Test Section," Proc. ICAPP'05, Seoul, Korea, May 15-19 (2005).

[6] H. Komita, S. Morooka, S. Yoshida, and H. Mori, "Study on the Heat Transfer to the Supercritical Pressure Fluid for Supercritical Water Cooled Power Reactor Development," Proc. NURETH-10, Seoul, Korea, October 5-9 (2003).

[7] J. D. Jackson and W. B. Hall, Forced Convection Heat Transfer to Fluids at Supercritical Pressure in Turbulent Forced Convection in Channels and Bundles, Vol. 2, 563-611, Hemisphere (1979).

[8] Y. Oka and K. Yamada, "Research and Development of High Temperature Light Water Cooled Reactor Operating at Supercritical-Pressure in Japan," Proc. ICAPP' 04, Paper 4233, Pittsburgh, PA USA, June 13-17 (2004).